SUPPLEMENTARY INFORMATION TO

Mechanisms and kinetics of CO_2 uptake on bicontinuous mesoporous silica modified with n-propylamine

Zoltán Bacsik[1], Nanna Ahlsten[2], Asraa Ziadi[2], Guoying Zhao[1], Alfonso E. Garcia-Bennett[3], Belén Martín-Matute[2], Niklas Hedin[1]*

[1]Department of Materials and Environmental Chemistry, Berzelii Center EXSELENT on Porous Materials, Arrhenius Laboratory, Stockholm University, SE-106 91 Stockholm, Sweden

[2]Department of Organic Chemistry, Berzelii Center EXSELENT on Porous Materials, Arrhenius Laboratory, Stockholm University, SE-106 91 Stockholm, Sweden

[3]Nanotechnology and Functional Materials, Department of Engineering Sciences, The Ångström Laboratory, Uppsala University, Box 534, SE-751 21 Uppsala, Sweden

niklas.hedin@mmk.su.se

Functionalization of AMS-6 with 3-aminopropyl triethoxysilane

AMS-6 was dried in an oven for 20 h at 150 °C before modification. A suspension of AMS-6 (300 mg) in toluene (18 mL) was stirred at 50 °C for 30 min under argon in a closed tube. The tube was opened and water (68 μL, 3.78 mmol) was added dropwise to the mixture. After resealing the tube, the mixture was heated to 120 °C for 1.5 h, after which 3-aminopropyltriethoxysilane (2.54 g, 11.4 mmol) was added to the mixture. When the addition was complete, the tube was closed and heated at 120 °C for 72 h. After cooling to room temperature, the tube was opened and the solid was filtered and washed with toluene (3 x 10 mL) and free residual 3-aminopropyltriethoxysilane was removed by soxhlet extraction in EtOH. The resulting solid was dried under reduced pressure over night. Anal. C,15.17; H, 3.67; N, 4.85. Functionalization with 3-aminopropylmethyldiethoxysilane was performed in a similar manner. Functionalization of MCM-48 3-aminopropyltriethoxysilane and 3-aminopropylmethyldiethoxysilane were performed in a similar manner.

Surface area of AMS-6 in a powder and pellet form

AMS-6. The adsorption isotherms measured on the powder and pellet were practically equivalent proving that no structural collapse of the pore system occurred due to the pellet pressing.

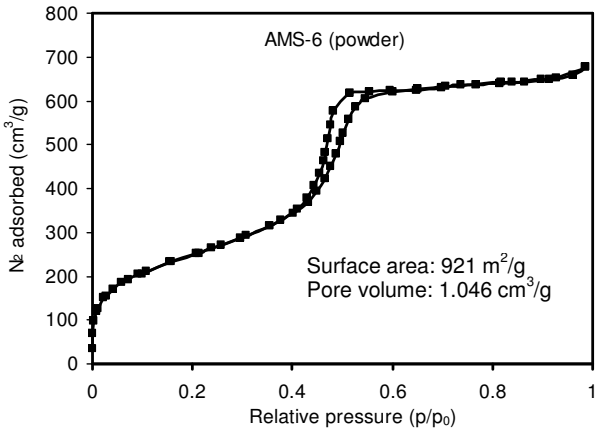

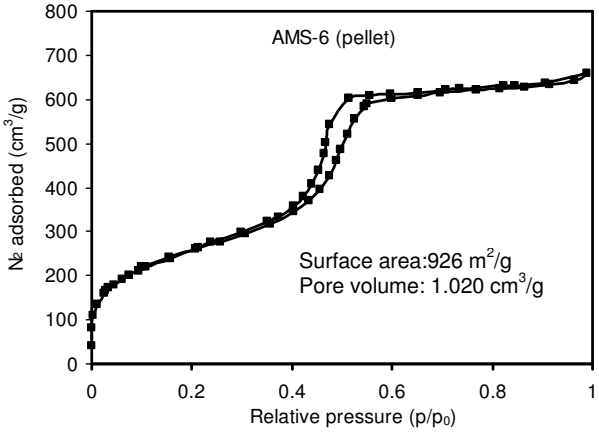

Table S1. Identification of the species formed by the reaction of CO_2 and immobilized amine groups with in situ IR spectroscopy

Reference	Adsorbent*	IR technique	Sample preparation	Model gas	Assignation, compounds (wavenumber in cm^{-1}) (No water present)	Assignation, compounds (wavenumber in cm^{-1}) (In the presence of water)
Tsuda, 1992	silica gel/APTES	Simple IR (no in situ)	No preparation	CO_2 in N_2	Ammonium carbamate (1580, 1330)	-
Chang, 2003	SBA-15/APTES	DRIFT	He flow, 25 ºC, 1h	4 % CO_2 in He, 2.5 % H_2O	bidentate bicarbonate (1634), bidentate carbonate (1575, 1390), monodentate bicarbonate (1493, 1432), monodentate carbonate (1335)	The same as in dry experiments.
Khatri, 2005	SBA-15/*N*-(2-aminoethyl)-3-aminopropyl	DRIFT	He flow, 30 ºC, 2h	10% CO_2, 4% H_2O in He	-	bidentate bicarbonate (1628), bidentate carbonate (1541), monodentate bicarbonate (1470, 1422), monodentate carbonate (1337), carbamic acid (1287), non-discussed band at around 1700 cm^{-1}
Khatri, 2006	SBA-15/APTES	DRIFT	N/A	10 % CO_2 and 4 % D_2O in Ar	-	Bicarbonates and carbonates (shifted band position due to hydrogen/deuterium isotope change)
Fisher, 2009	B Zeolite/TEPA	DRIFT	He flow, 135 ºC, 0.5h	10 % CO_2 in Ar	bidentate carbonate (1564, 1390), monodentate bicarbonate (1470) monodentate carbonate (1313)	-
Tanthana, 2010	TEPA/SiO_2	DRIFT	Ar flow, 55 ºC	15% CO_2, 4% H_2O in air	-	CO_2-H_2N- (2627), carbamic acid (1680), carbamate (1520), carboxylate (1430), carboxylate and carbamate (1315)
Hao, 2010	Silica (AMS)/APTES	N/A	N/A	N/A	NH stretch in carbamate (3410), NH_3^+ def in carbamate (1632), C=O stretch in carbamate (1563), NCOO (1484),	-
Leal, 1995	Silica gel/APTES	Transm.	150 ºC, 2 h	10 Torr dry and humid CO_2	Carbamate (1411), bicarbonate (1385)	The ratio of carbamate (1411) and bicarbonate (1385) changes compare to dry CO_2
Huang, 2003	MCM-48/APTES	Transm.	He-flow, N/A	5% CO_2 in He	Bicarbonate (1382)((after Leal et al.)), C=O asym. Stretch (1432, 1485) in carbamate, C-O stretch and NH_3^+ def. (1560), NH_3^+ def (1635)	Higher overall intensity of the same bands as in case of dry CO_2
Wang, 2009	SBA-15/PEI	Transm.	He flow, 80 ºC, 2h	For moist CO_2 runs: preadsorption of water	NH_3^+ def (1630) and C=O stretch (1520) and NCOO (1410, 1320) in carbamate, chemisorbed CO_2 (2450, 2160)	Slightly higher uptake, same bands as in case of dry CO_2, no bicarbonate formation observed

Zheng, 2005	SBA-15/Ethylene diamine	Transm.	Ar flow, 135 ºC	Pure CO_2 and CO_2/ 2 % H_2O	NH_2^+, NH def, C-N (1576) in intramolecular carbamate	The same bands as in case of dry CO_2
Hiyoshi, 2005	SBA-15/APTES	Transm.	He flow, 150 ºC, 1h	3% CO_2, in He, and 3% CO_2, 2 % H_2O in He	NH stretch (3439) and NH_3^+ (1630) and C=O stretch (1563) and NCOO (1488) in carbamate	The same bands as in case of dry CO_2
Knöfel, 2009	Amorph. Silica/APTES	Transm.	Evacuation $<10^{-7}$ mbar, 160 ºC, overnight	Pure CO_2 (?)	NH stretch (3435), NH_3^+ (1626), COO^- asym (1545), NH_3^+ (1487) bend and COO^- sym (1381) in carbamate, C=O stretch in carbamic acid (1680) Faster formation of carbamic acid observed.	-
Bacsik, 2010	Mesocaged silica/APTES	Transm.	Evacuation $<10^{-6}$ Torr, 140 ºC, 6h	100 % CO_2	Physisorbed linear CO_2 (2340); NH stretch (3440), NH_3^+ (1626), COO^- asym (1567), NH_3^+ (1500) $NCOO^-$ (1381) in carbamate; C=O stretch in carbamic acid (~1701)	-
Danon, 2011	SBA-15/APTES with different surface coverages	DRIFT	Evacuation $<10^{-7}$ Torr, 100 ºC	Pure CO_2, 20 Torr	Physisorbed linear CO_2 (2340); NH_3^+ (1625), COO^- asym (1564), NH_3^+ (1485-1550) $NCOO^-$ (1335-1430) in carbamate; C=O stretch in carbamic acid (~1701)	-
This study	MCM-48/APTES AMS-6/APTES	Transm.	Evacuation $<10^{-6}$ Torr, 140 ºC, 6h	20 V/V% CO_2 in N_2, the same saturated with H_2O	NH str. (3440), NH_3^+ (1630), COO^- asym (1564), NH_3^+ (1484) bend. and COO^- sym (1433), C=O stretch in H-bonded carbamic acid (1680-1700), C=O stretch (1715) in carbamic acid silyl ester (See Table 2 in the paper for more details)	Carbamic acid silyl ester does not form; the ammonium carbamate ion par formation is enhanced in the present of water.

* In many studies there are more than one adsorbent investigated, here we refer the selected one(s) (silica support/amine)

FIGURES

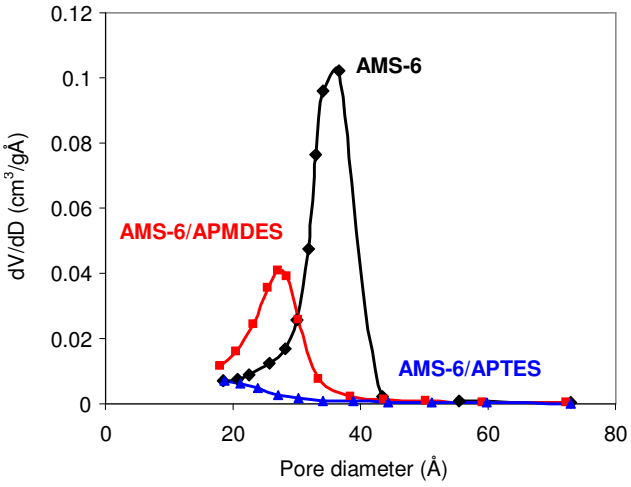

Figure S1A. Pore volume distribution in unmodified AMS-6, AMS-6/APMDES and AMS-6/APTES. The pore volume distribution (BJH model, desorption) is shifted towards smaller average pore dimensions as the degree of functionalization is increasing.

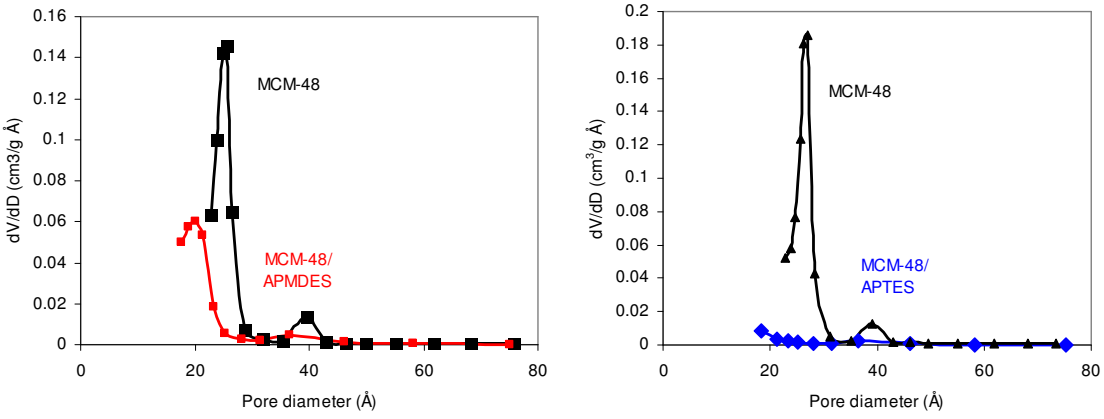

Figure S1B. Pore volume distribution in unmodified MCM-48, MCM-48/APMDES and MCM-48/APTES. The pore volume distribution (BJH model, desorption) is shifted towards smaller average pore dimensions as the degree of functionalization is increasing.

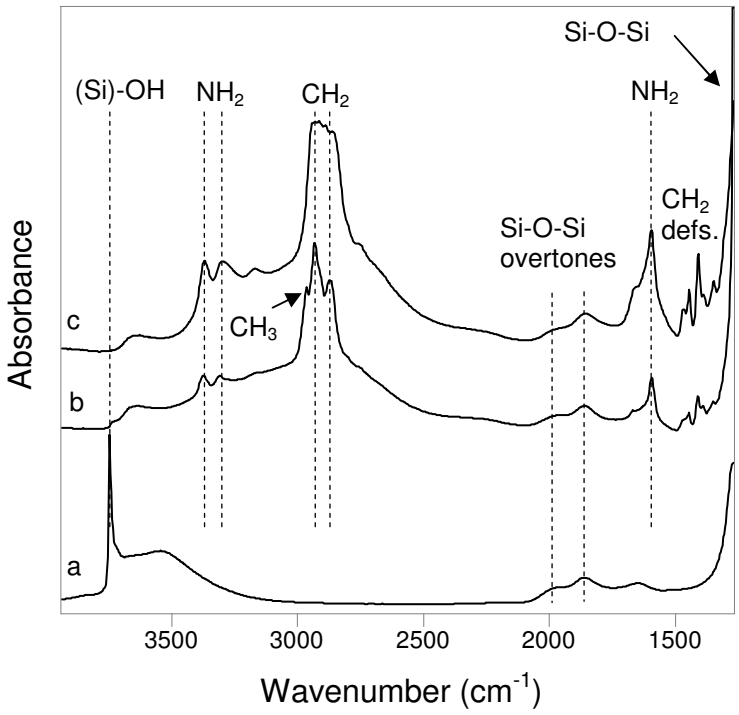

Figure S2. FTIR spectra of the a) AMS-6, b) AMS-6/APMDES and c) AMS-6/APTES. The spectra were measured in vacuum (<10^{-6} Torr) after pretreatment (140 ºC, <10^{-6} Torr, 6 h) of the self-supporting pellets. An empty cell was used as background.

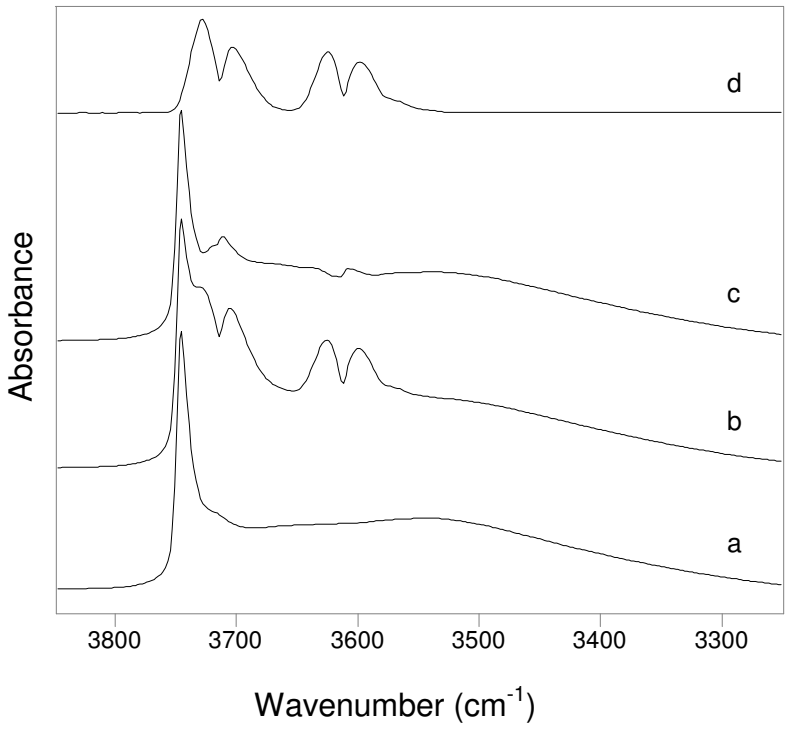

Figure S3. FTIR spectra of AMS-6 material a) measured in near vacuum conditions (<10^{-6} Torr) after heat treatment at 140 ºC, b) contacted with 760 Torr of pure CO_2, c) after subtraction of the corresponding gaseous reference spectrum for CO_2 and (d) the corresponding gaseous reference spectrum for CO_2.

Spectra were measured at room temperature and the background spectrum was recorded in the empty cell. The changes in the OH-stretchings could not be detected when using this particular background spectrum.

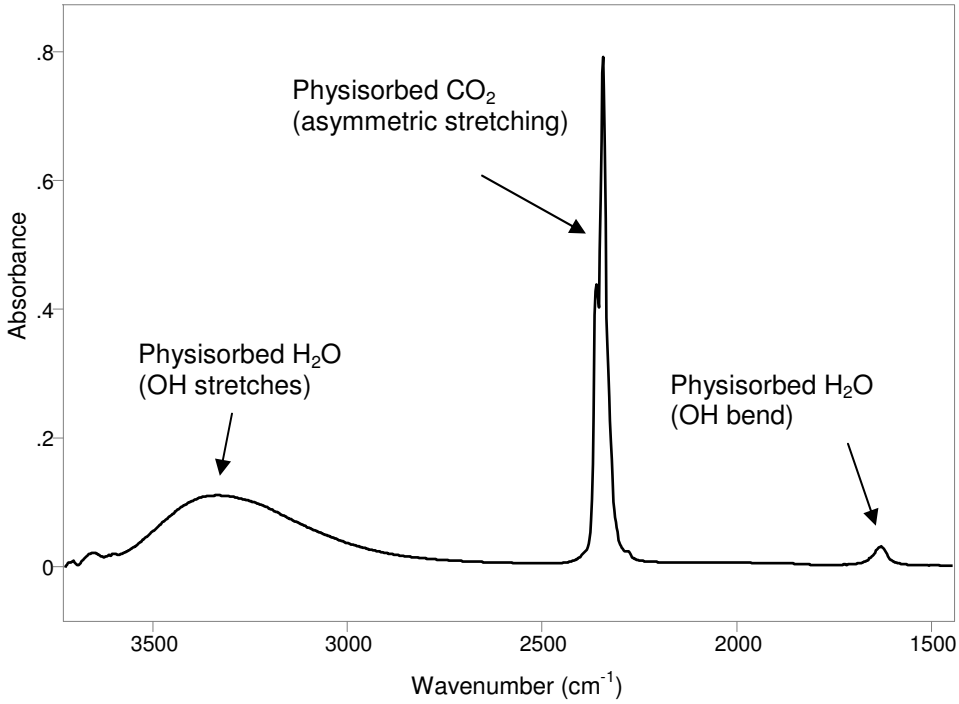

Figure S4. In situ FTIR spectrum of the adsorbed species on AMS-6 equilibrated with 400 Torr pure CO_2 saturated with water (2.1 V/V %). No carbonates or bicarbonates were observed.

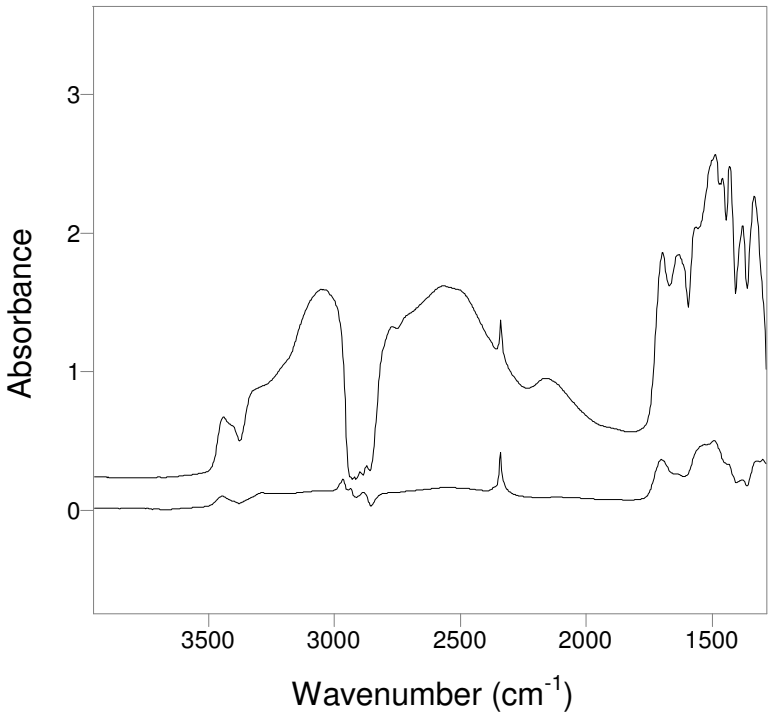

Figure S5. In situ FTIR spectra for AMS-6/APMDES and AMS-6/APTES contacted with 100 Torr of pure CO_2.

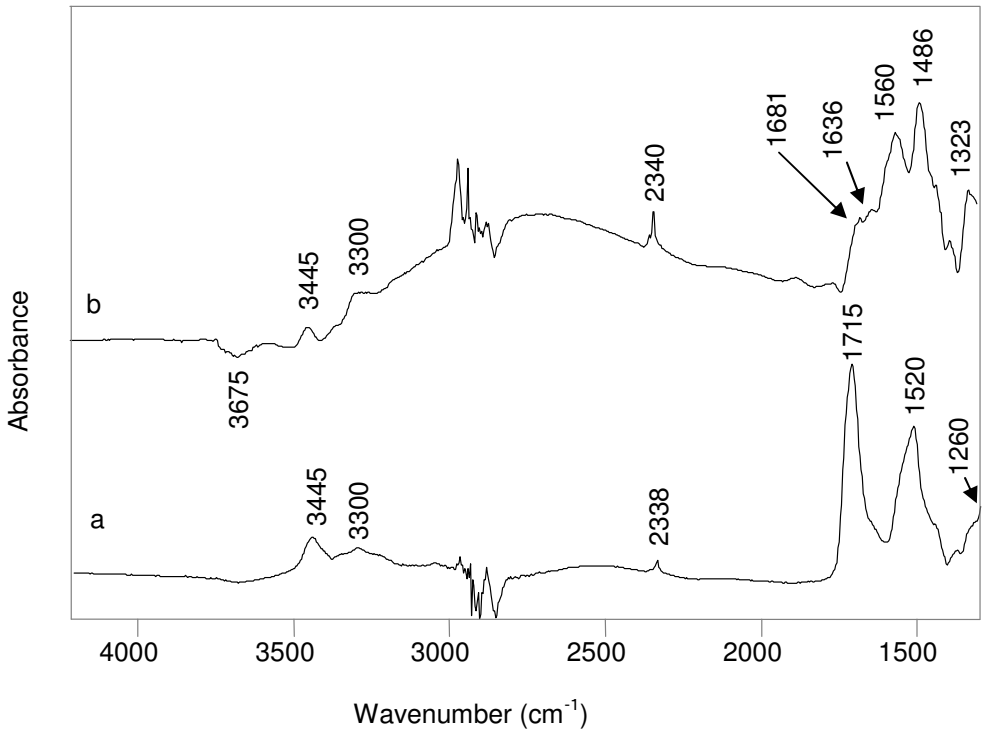

Figure S6. Differential IR spectra of the two major species form at different reaction rates during the adsorption of CO_2 on AMS-6/APMDES material: a) represents mainly silylpropylcarbamate. It is the difference spectrum of adsorbed species at 50 Torr CO_2 (20 V/V% in N_2) measured after 2 and 25 minutes (equilibrium); b) represents mainly propylammonium propylcarbamate and hydrogen bonded carbamic acid. It is the difference spectrum of the 50 Torr equilibrium spectrum and the difference spectrum Figure 8a (residual).

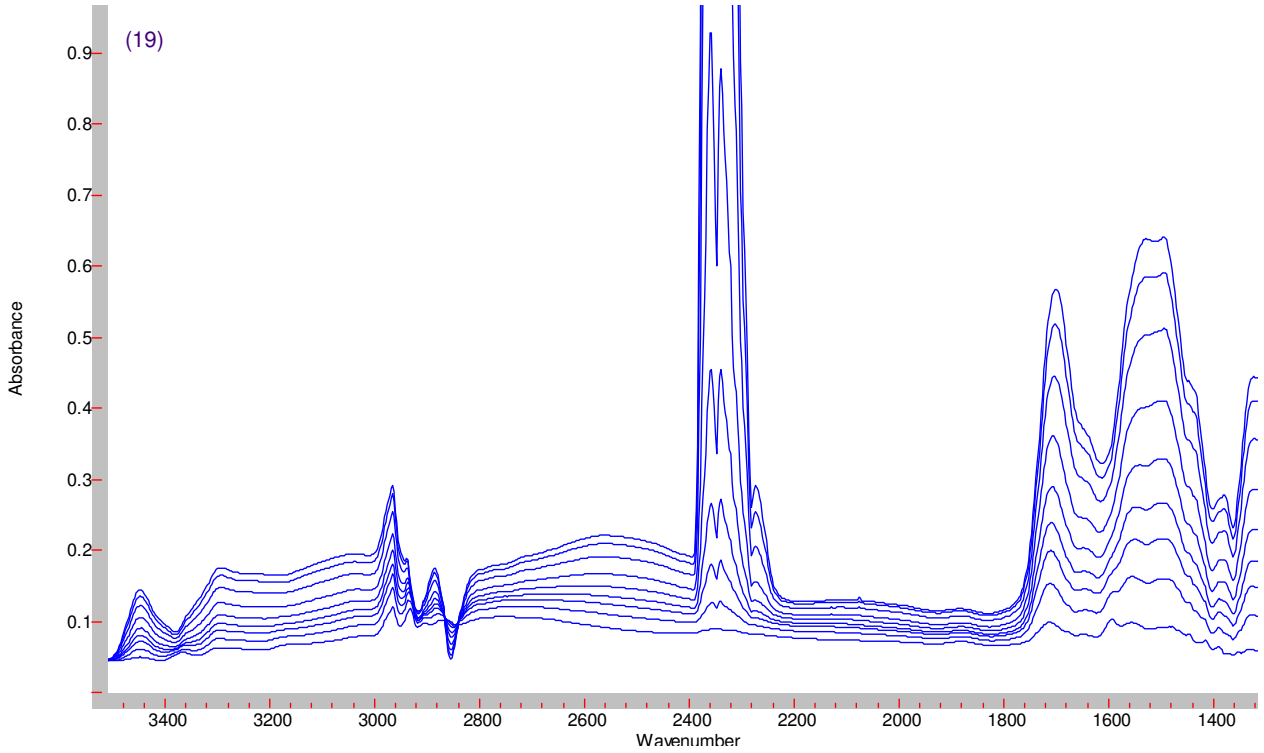

Figure S7A. ADSORPTION AMS-6/APMDES, **DRY** CO_2 in N_2, 2, 10, 25, 50, 100, 200, 400, 600, 760 Torr pressures (from bottom to top).

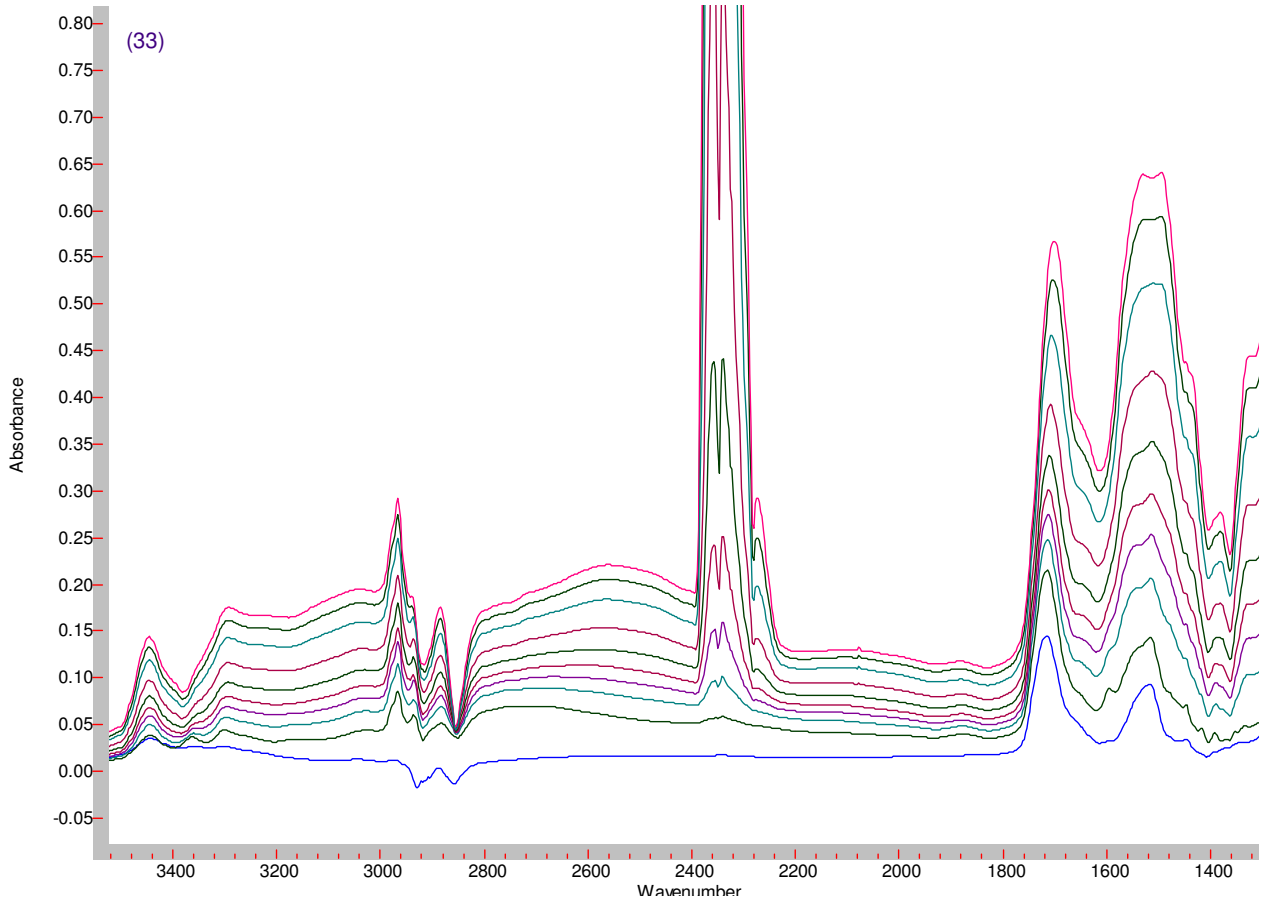

Figure S7B. DESORPTION AMS-6/APMDES **DRY** 20 % CO_2 in N_2 pressure 760, 600, 400, 200, 100, 50, 25, 10, 1 Torr, 30 min evacuation (from top to bottom)

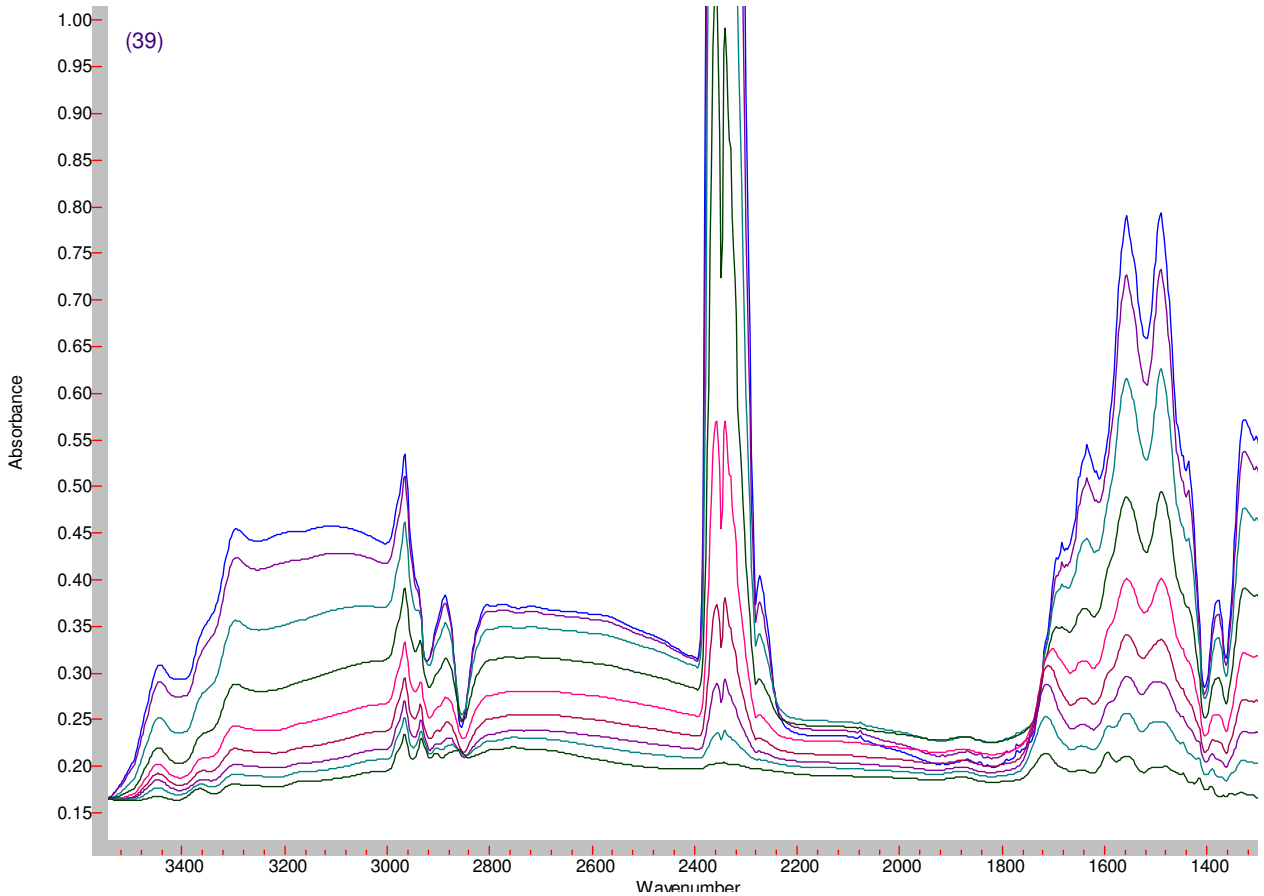

Figure S7C. ADSORPTION AMS-6/APMDES, **HUMID** CO_2 in N_2, 2, 10, 26, 50, 100, 200, 400, 600, 760 Torr pressures (from bottom to top)

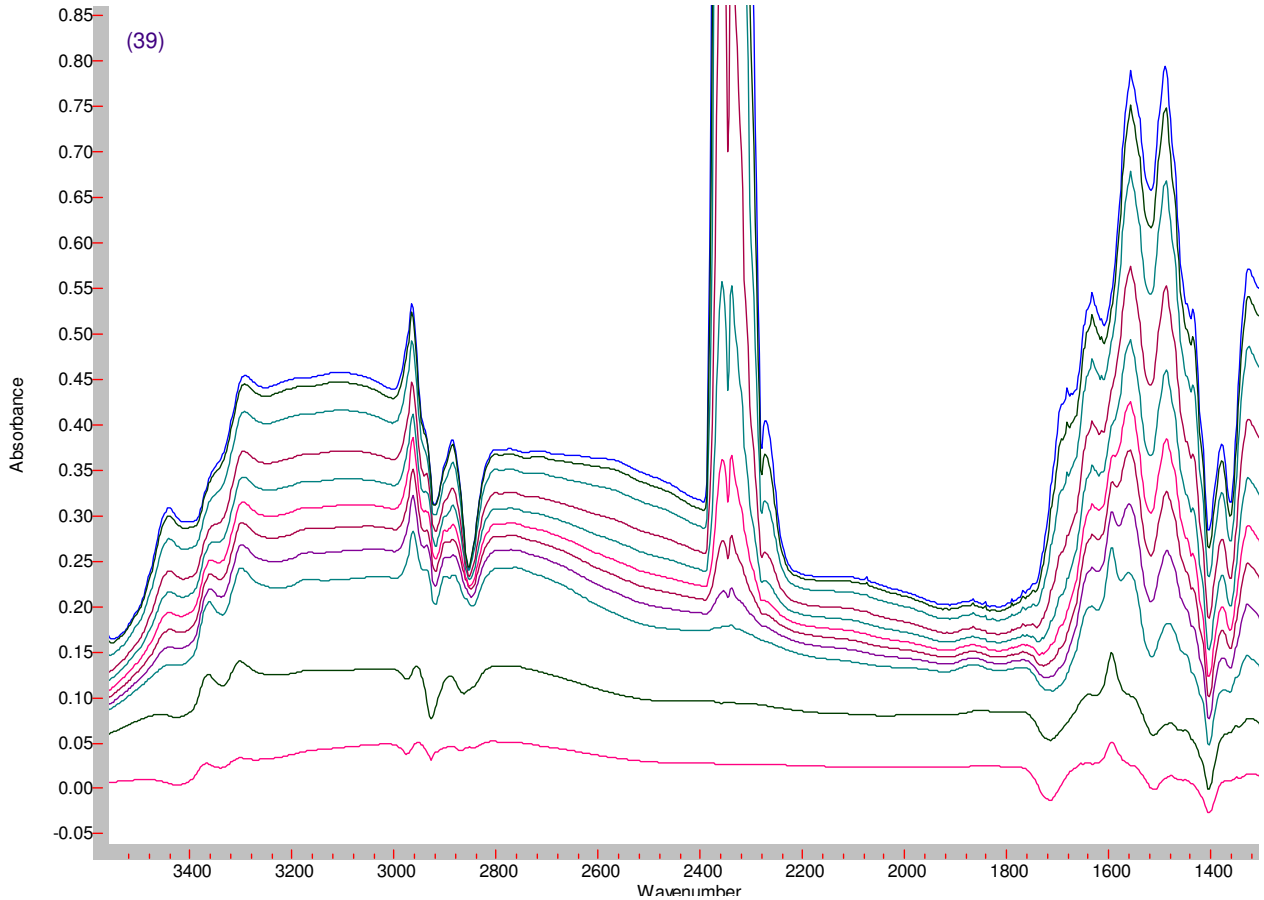

Figure S7D. DESORPTION AMS-6/APMDES **HUMID** 20 % CO_2 in N_2 pressure 760, 600, 400, 200, 100, 50, 25, 10, 2 Torr, 30 min evacuation, after heat treatment (from top to bottom)

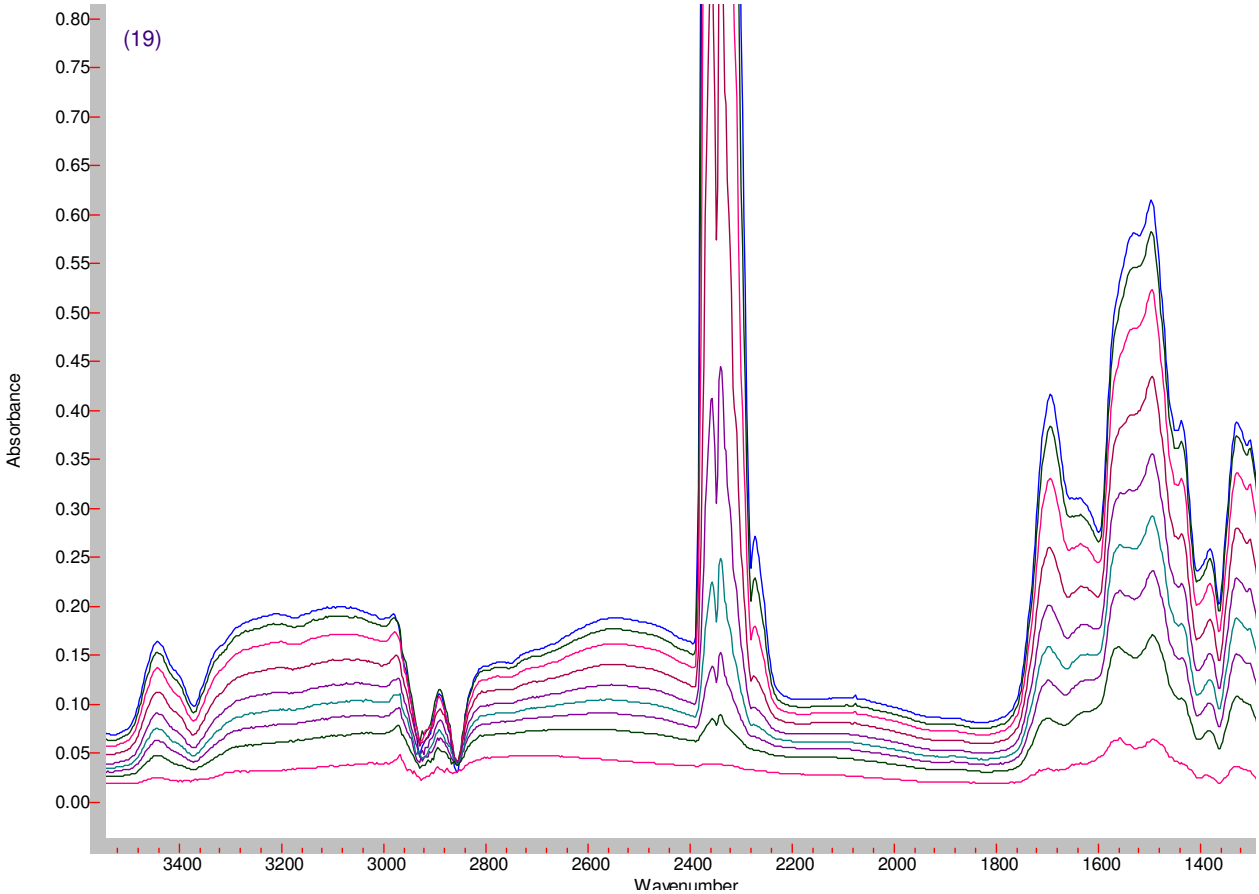

Figure S8A. ADSORPTION MCM-48/APMDES **DRY** 20 % CO_2 in N_2 pressure 1, 10, 25, 50, 100, 200, 400, 600, 760 Torr (from bottom to top)

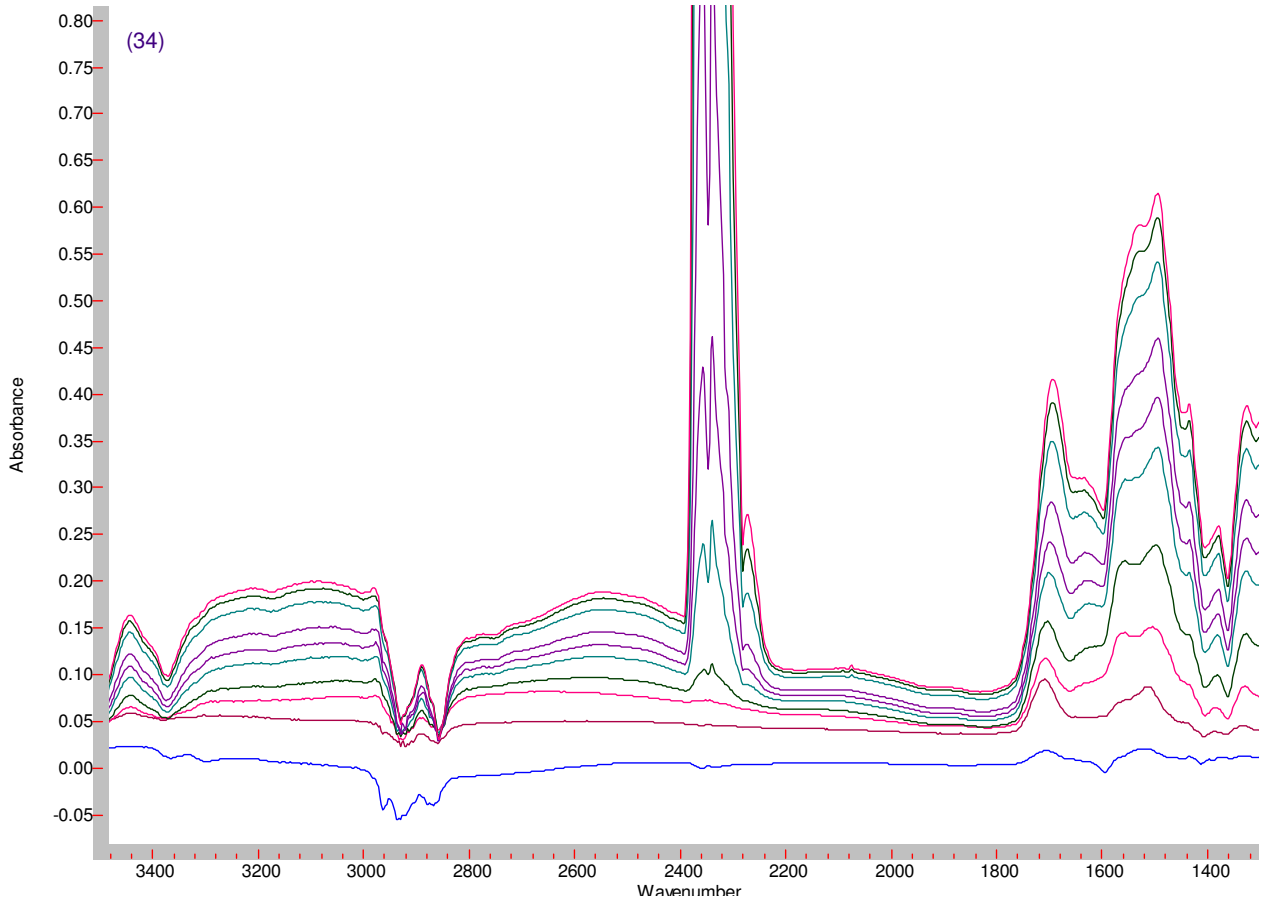

Figure S8B. DESORPTION MCM-48/APMDES **DRY** 20 % CO_2 in N_2 pressure 760, 600, 400, 200, 100, 50, 10, 1 Torr, 30 min evacuation, after heat treatment (from top to bottom)

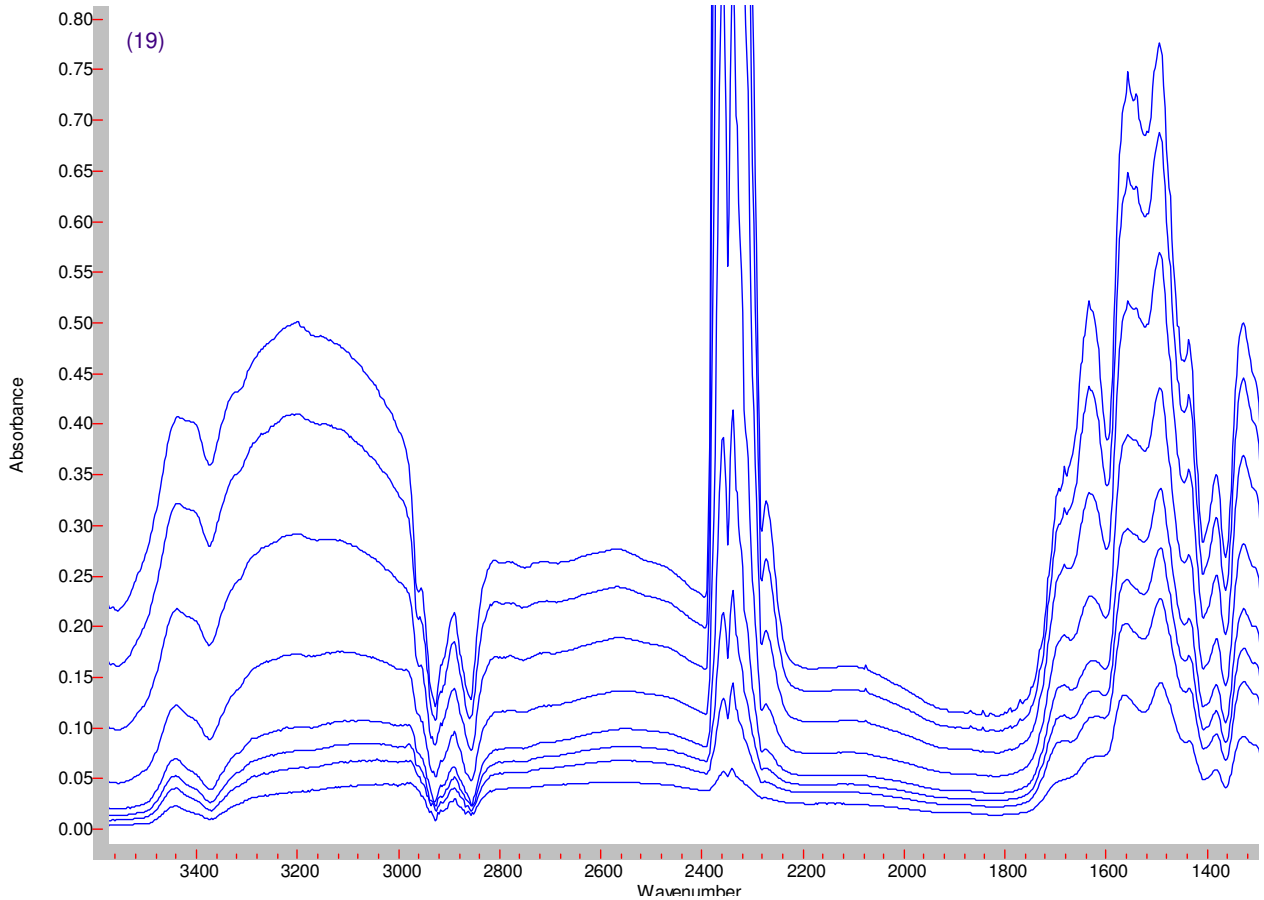

Figure S8C. ADSORPTION MCM-48/APMDES **HUMID** 20 % CO_2 in N_2 pressure 8, 30, 54, 100, 200, 400, 600, 760 Torr (from bottom to top)

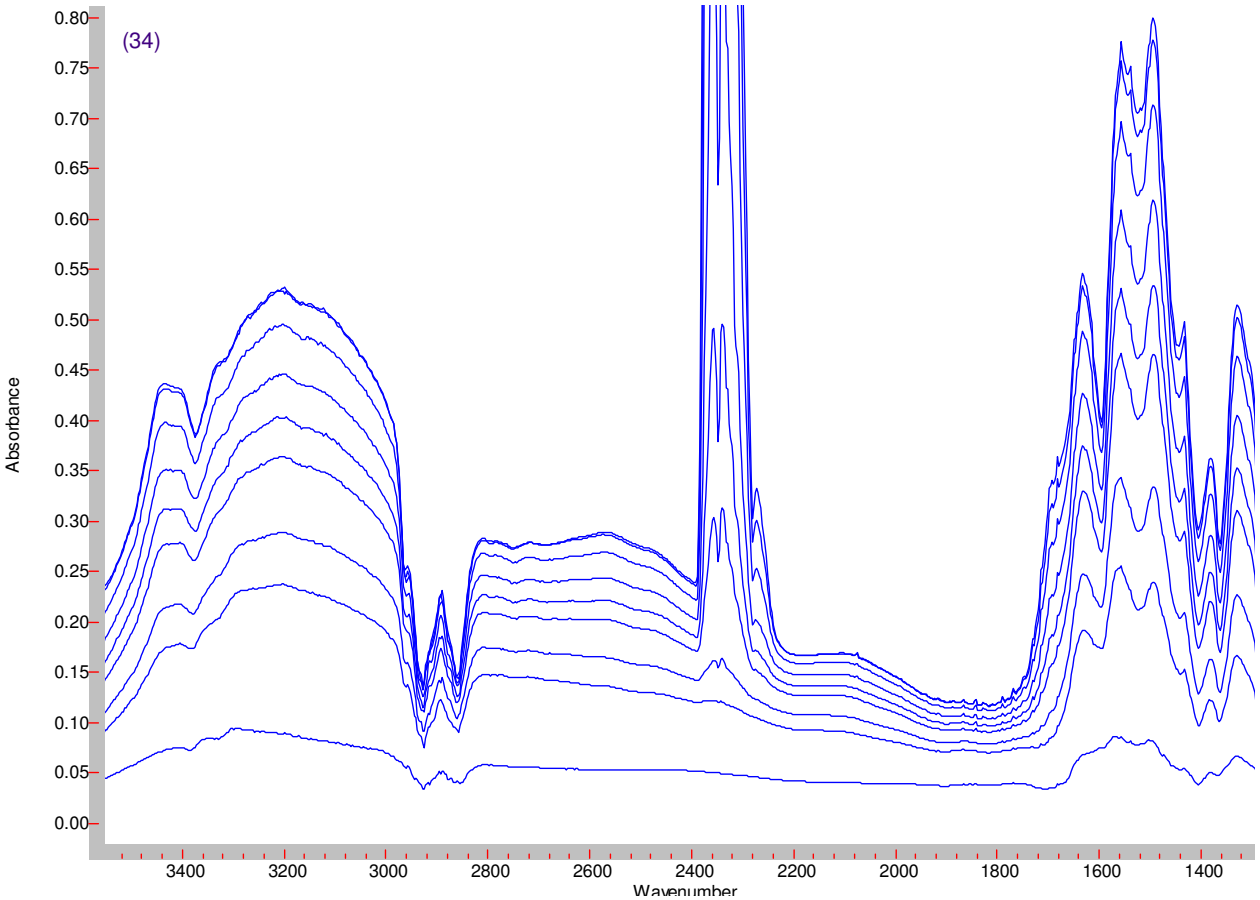

Figure S8D. DESORPTION MCM-48/APMDES **HUMID** 20 % CO_2 in N_2 pressure 760, 600, 400, 200, 100, 50, 10, 1 Torr, 30 min evacuation, (from top to bottom)

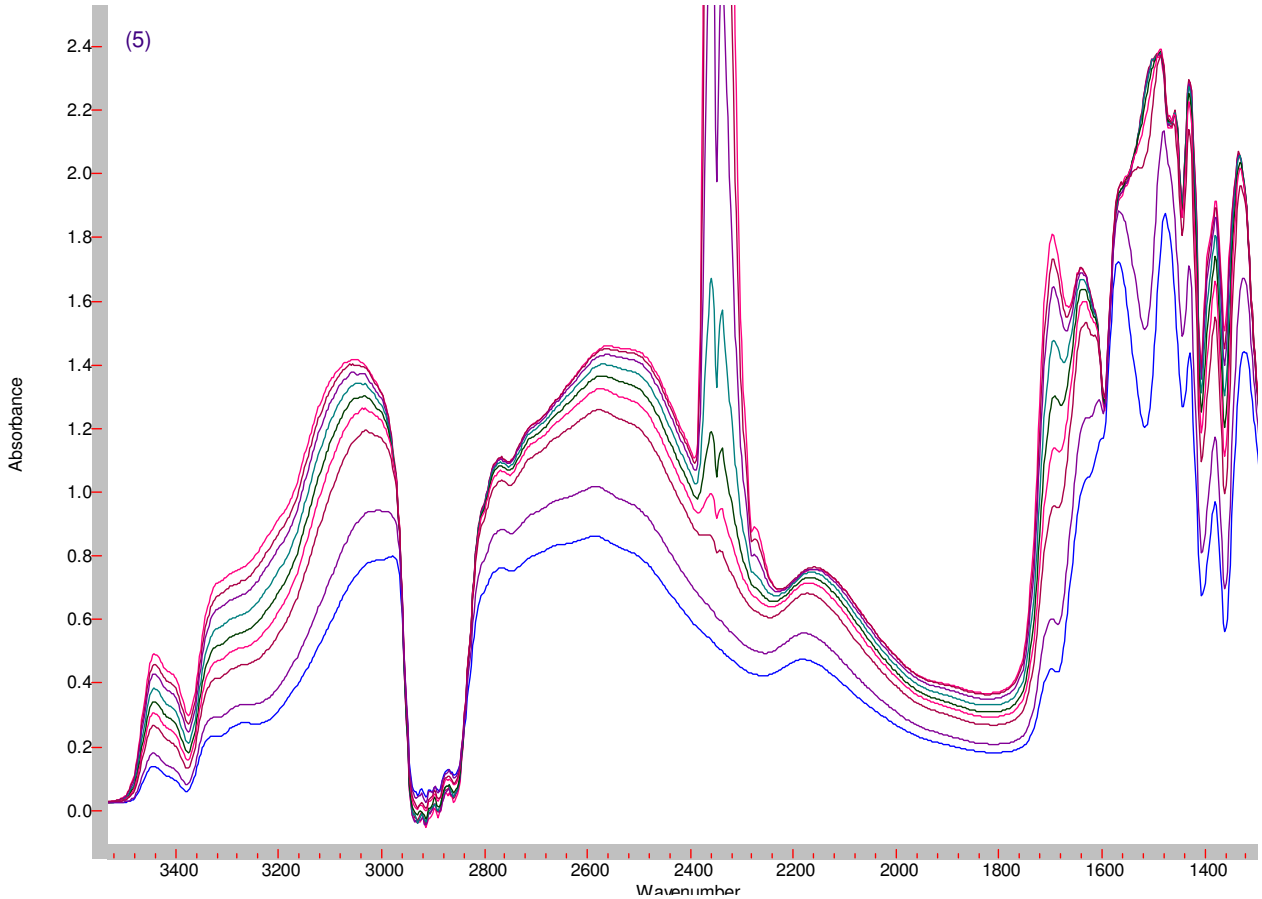

Figure S9A. ADSORPTION AMS-6/APTES **DRY** 20 % CO_2 in N_2 pressure 5.6, 13, 27, 55, 100, 200, 400, 600, 760 Torr (from bottom to top)

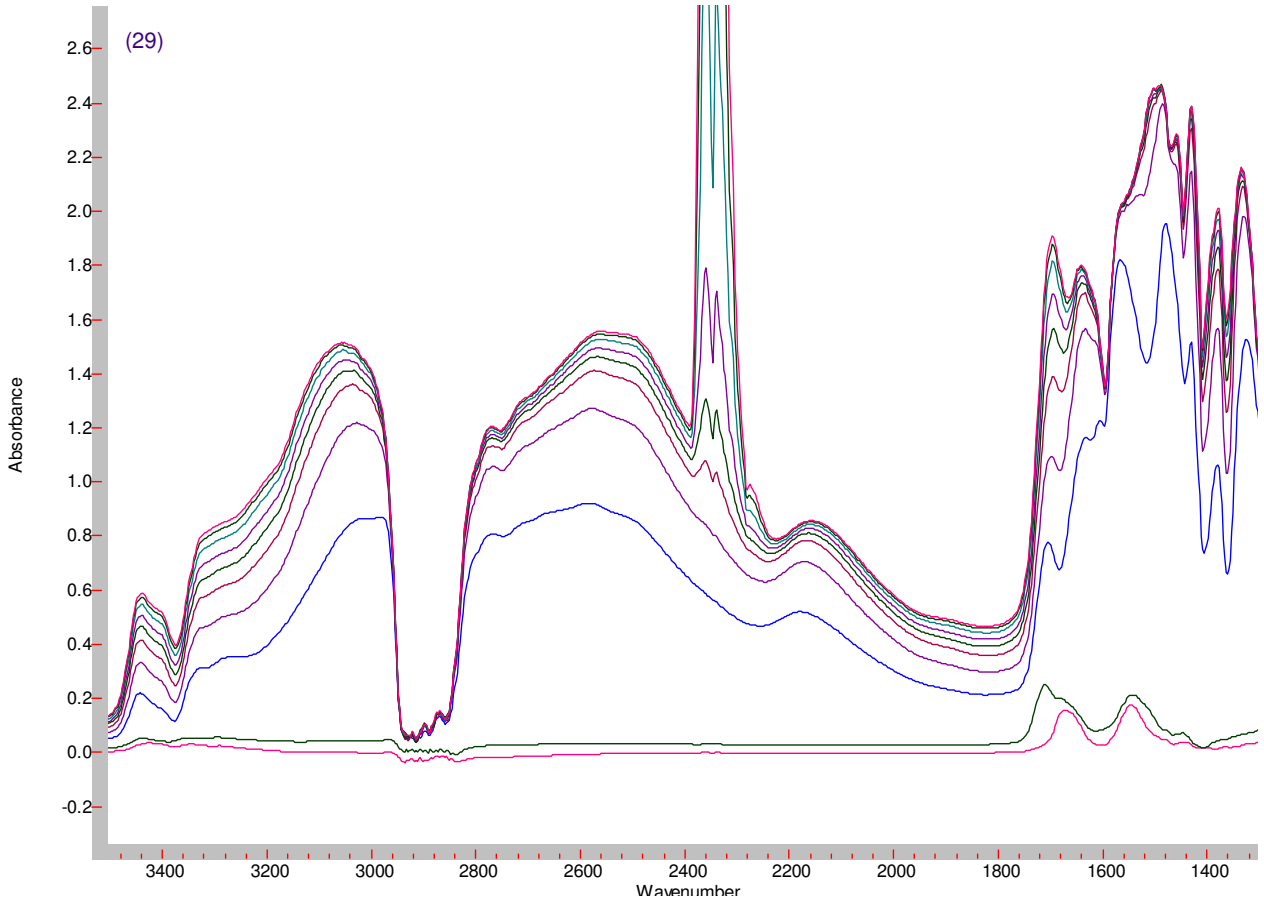

Figure S9B. DESORPTION AMS-6/APTES **DRY** 20 % CO_2 in N_2 pressure 760, 600, 400, 200, 100, 50, 25, 10, 2 Torr, 30 min evacuation, heat treatment (from top to bottom)

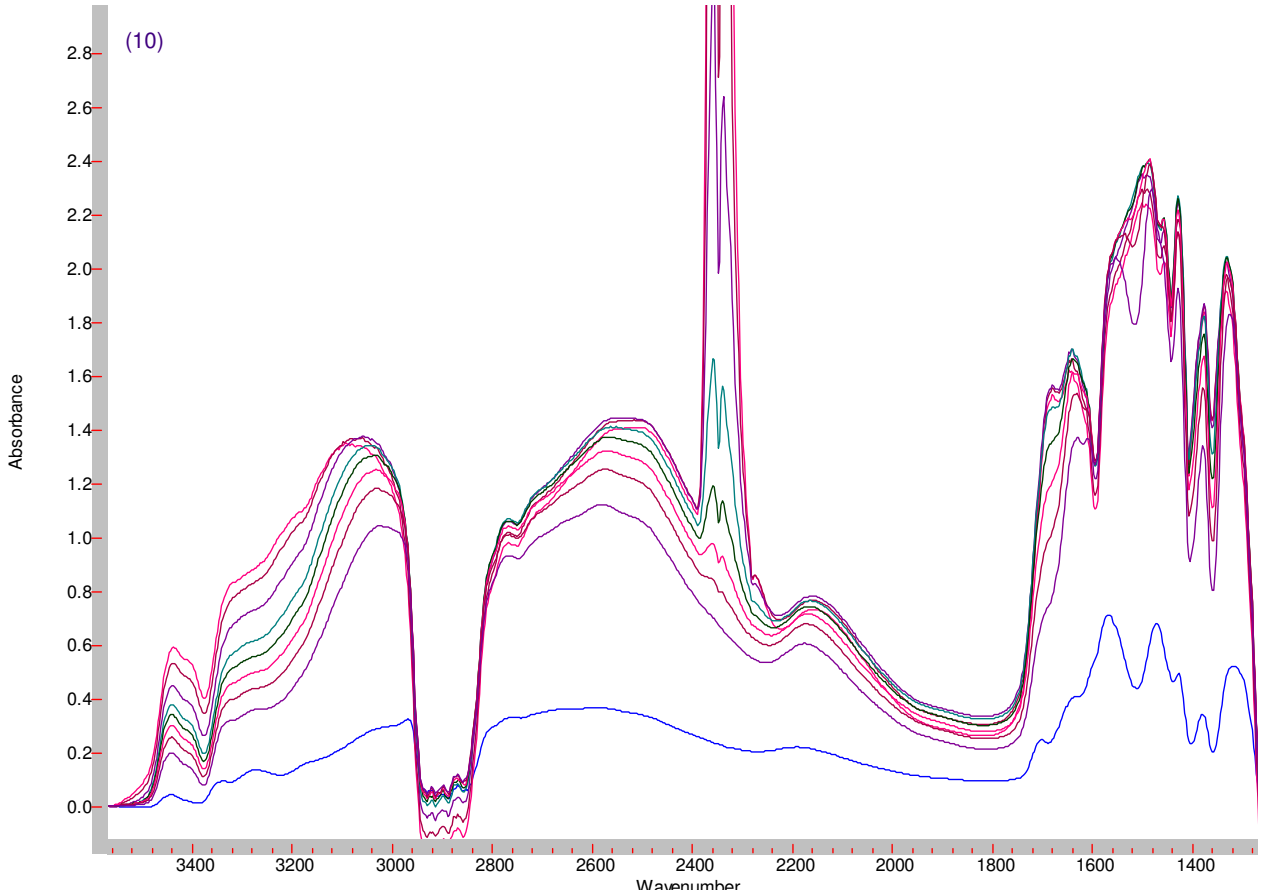

Figure S9C. ADSORPTION AMS-6/APTES **HUMID** 20 % CO_2 in N_2 pressure 1, 10, 25, 50, 100, 200, 400, 600, 760 Torr (from bottom to top)

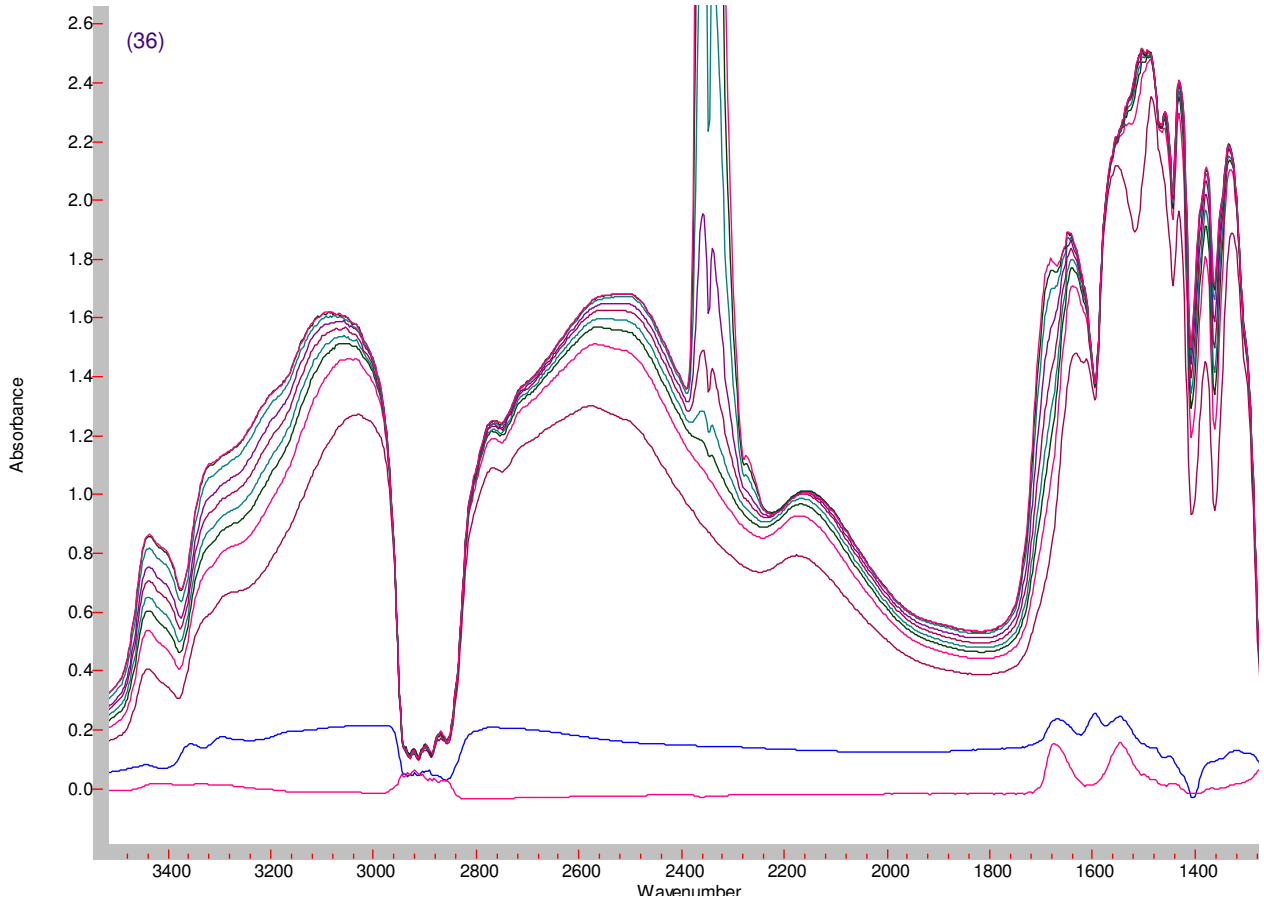

Figure S9D. DESORPTION AMS-6/APTES **HUMID** 20 % CO_2 in N_2 pressure 760, 600, 400, 200, 100, 50, 24, 10, 1 Torr, 30 min evacuation, heat treatment (from top to bottom)

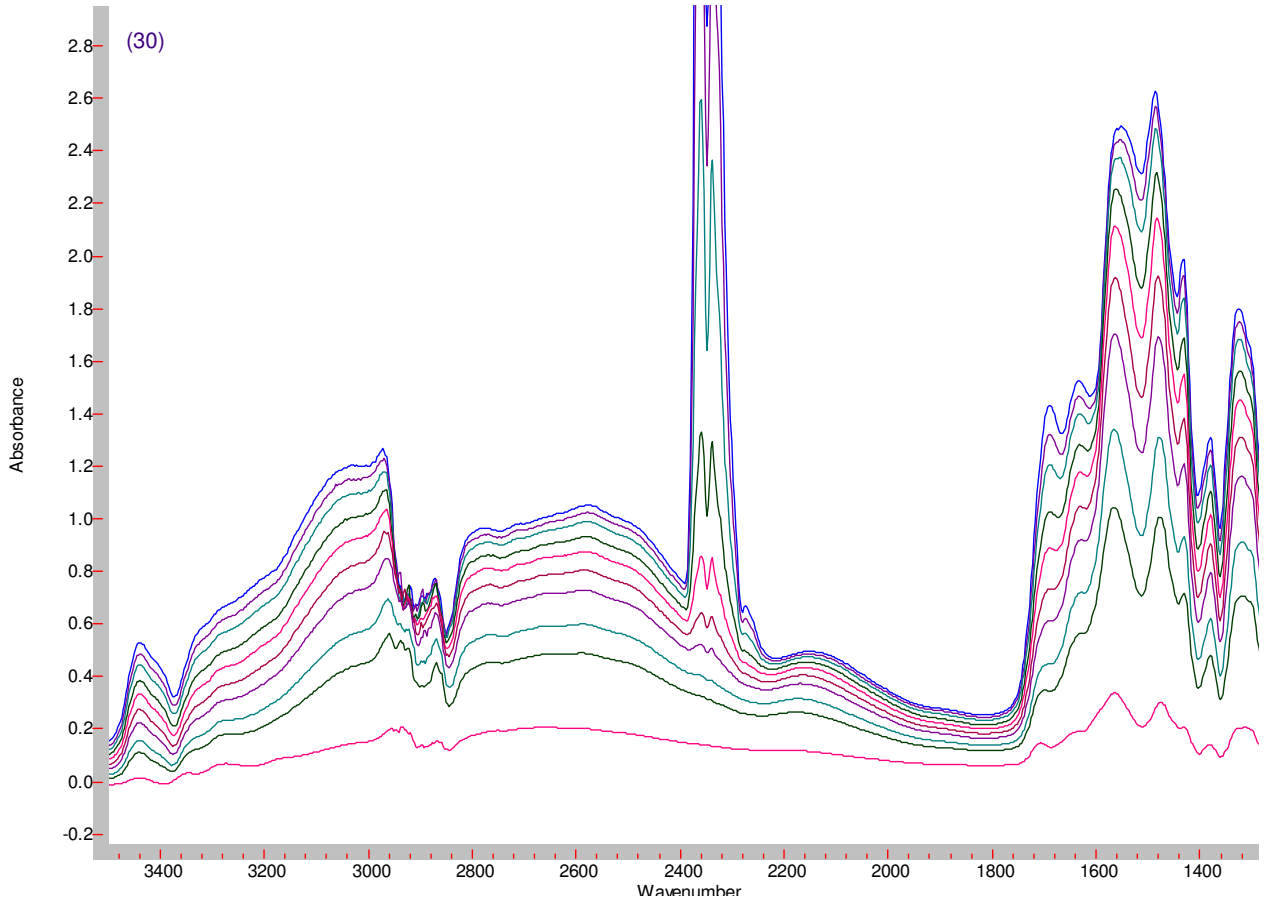

Figure S10A. ADSORPTION MCM-48/APTES **DRY** 20 % CO_2 in N_2 pressure 1, 5, 10, 25, 50, 100, 200, 400, 600, 760 Torr (from bottom to top)

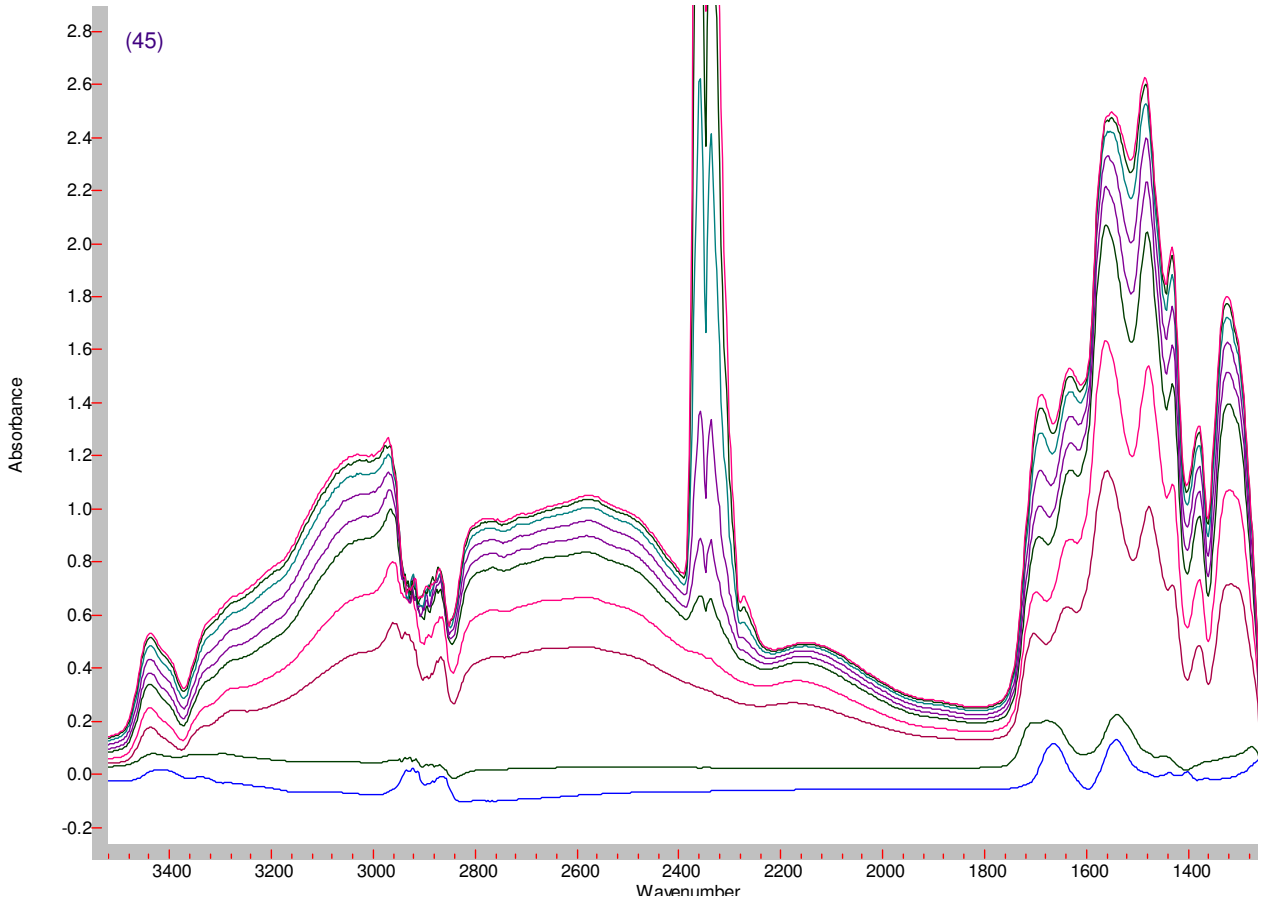

Figure S10B. DESORPTION MCM-48/APTES **DRY** 20 % CO_2 in N_2 pressure 760, 600, 400, 200, 100, 50, 10, 2 Torr, 30 min evacuation, heat treatment (from top to bottom)

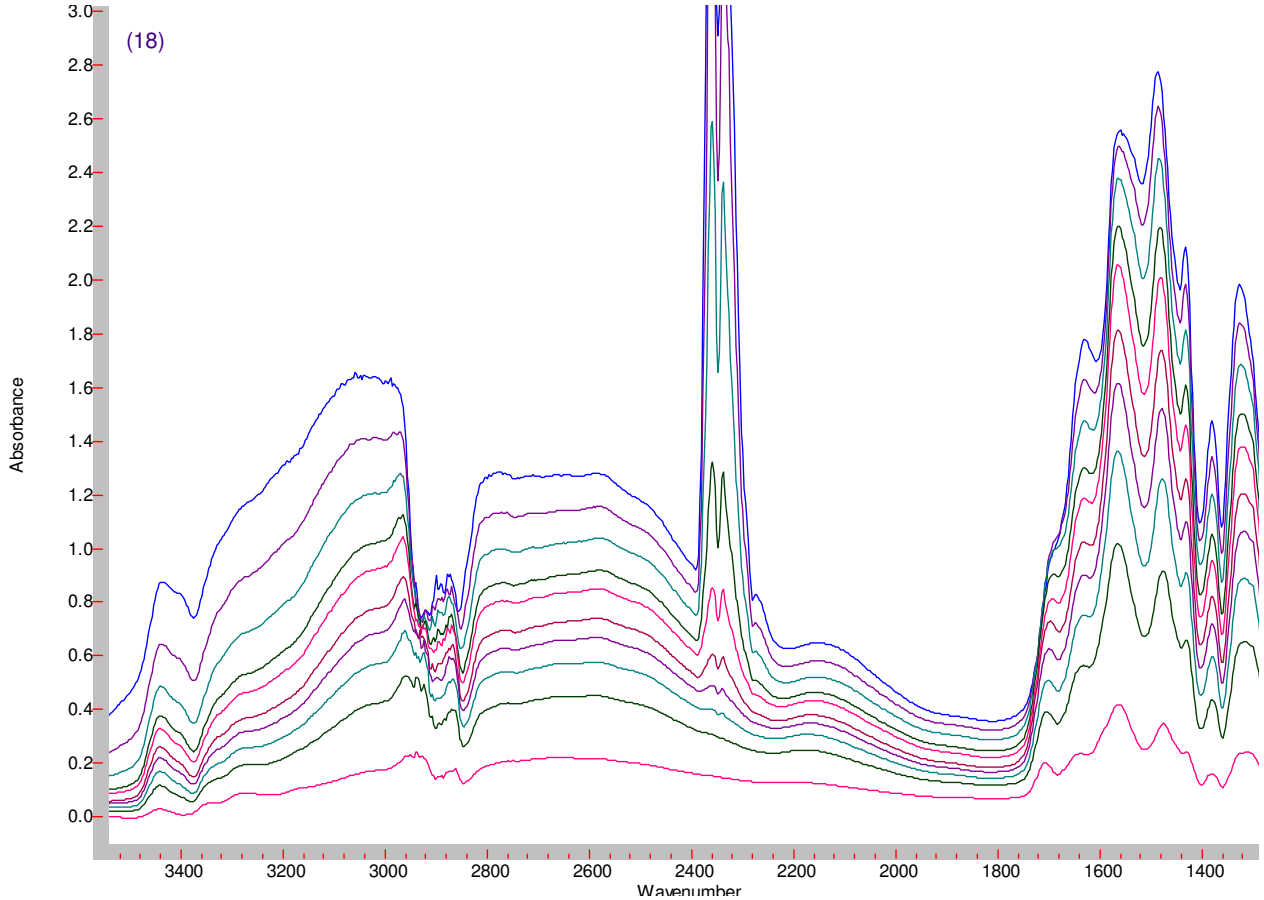

Figure S10C. ADSORPTION MCM-48/APTES **HUMID** 20 % CO_2 in N_2 pressure 1, 5, 13, 25, 50, 100, 200, 400, 600, 760 Torr (from bottom to top)

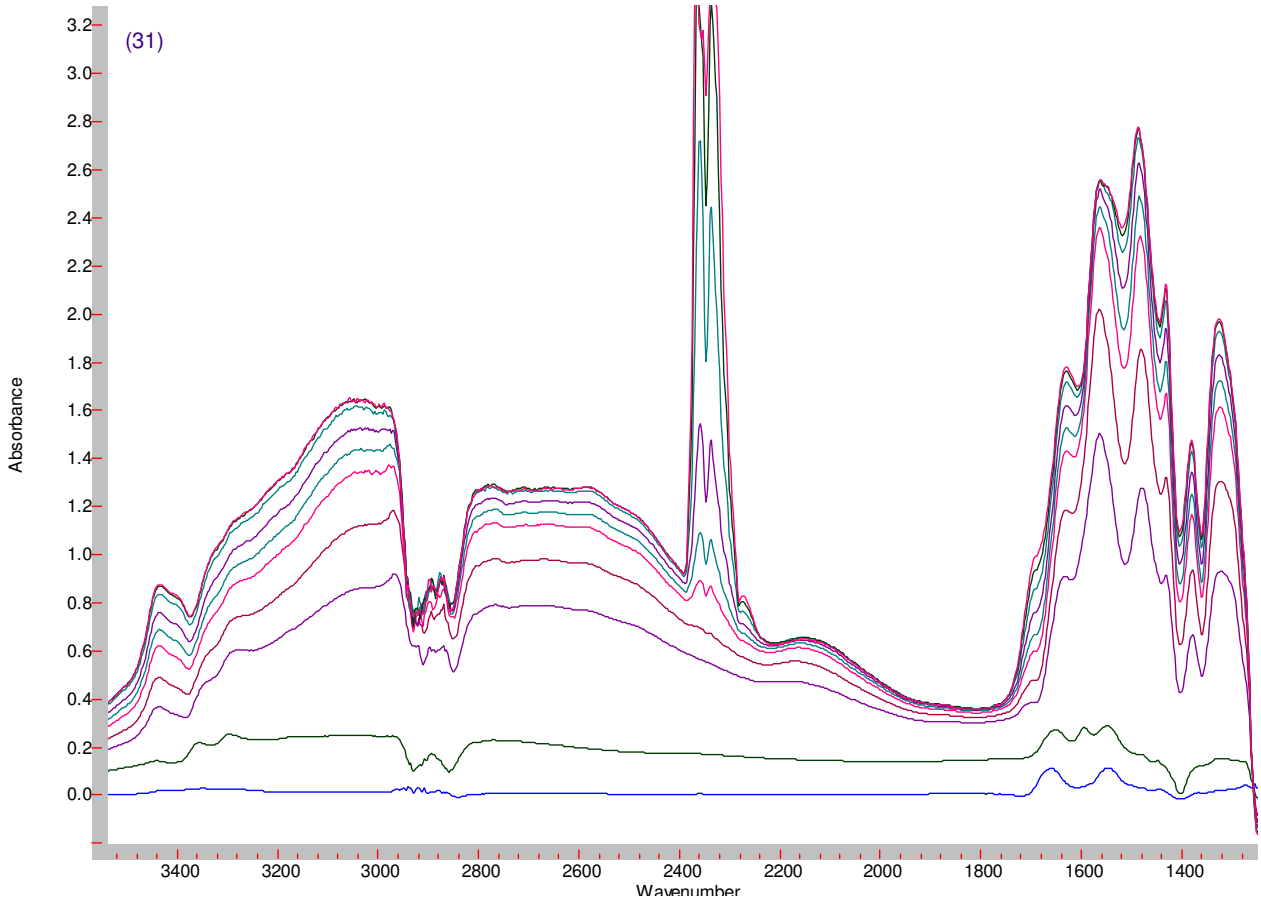

Figure S10D. DESORPTION MCM-48/APTES **HUMID** 20 % CO_2 in N_2 pressure 760, 600, 400, 200, 100, 50, 10, 2 Torr, 30 min evacuation, heat treatment (from top to bottom)

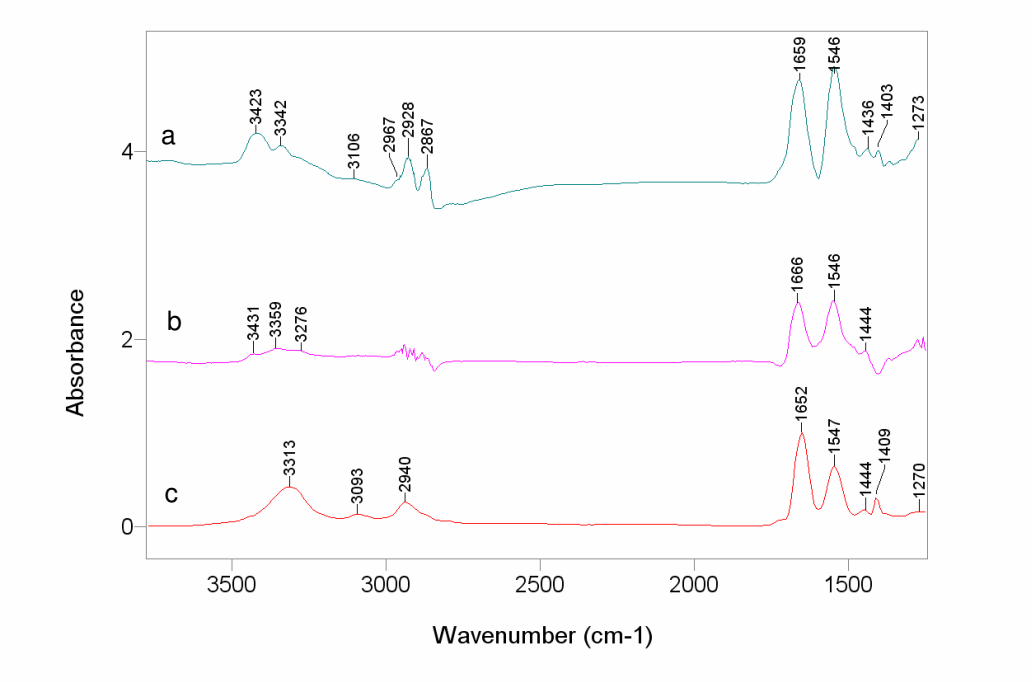

Figure S11A. The IR spectra of remained species on MCM-48/APTES after a) dry and b) moist CO_2 adsorption and heat (140 °C, 6h) regeneration; c) poly (N-methyl acryl amide) reference spectrum

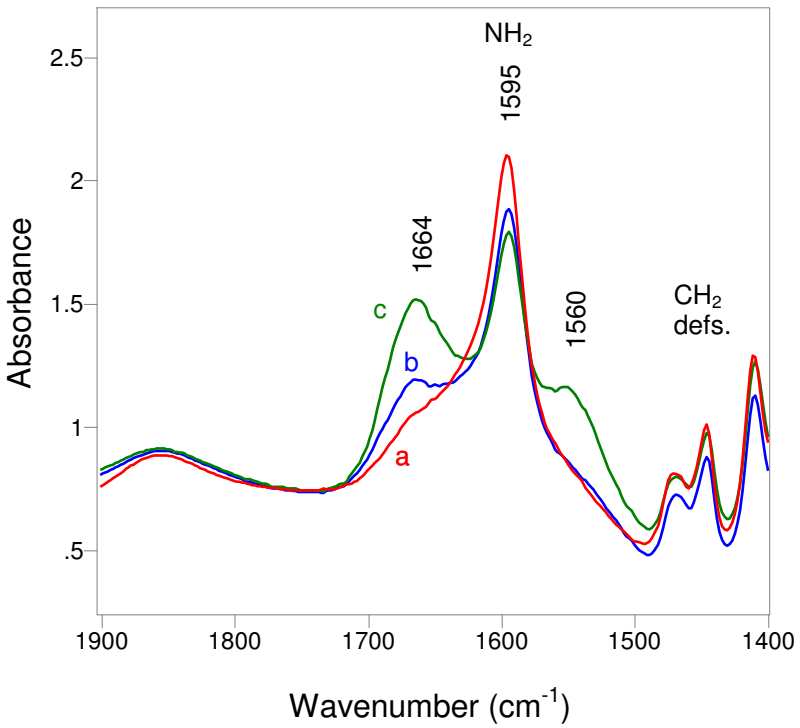

Figure S11B. IR spectra of the fresh (a) MCM-48/APTES and after 3 (b) and 6 (c) cycles of CO_2 uptake. A spectrum in from an empty cell was used when recording the single beam spectrum for further use as a background spectrum.

References in the supplementary information

Hicks, J. C.; Drese, J. H.; Fauth, D. J.; Gray, M. L.; Qi, G. G.; Jones, C. W. *J. Am. Chem. Soc.* **2008**, *130*, 2902-2903.

Gray, M. L.; Soong, Y.; Champagne, K. J.; Pennline, H. W.; Baltrus, J.; Stevens Jr., R. W.; Khatri, R.; Chuang, S. S. C. *Int. J. Environ. Technol. Manage.* **2004**, *4*, 82-88.

Chang, A. C. C.; Chuang, S. S. C.; Gray, M.; Soong, Y. *Energy Fuels* **2003**, *17*, 468-473.

Harlick, P. J. E.; Sayari, A. *Ind. Eng. Chem. Res.* **2007**, *46*, 446-458.

Serna-Guerrero, R.; Dana, E.; Sayari, A. *Ind. Eng. Chem. Res.* **2008**, *47*, 9406-9412.

Danon, A.; Stair, P. C.; Weitz, E. *J. Phys. Chem. C* **DOI:** 10.1021/jp200914v

Kim, S.; Ida, J.; Guliants, V. V.; Lin, J. Y. S. *J. Phys. Chem. B* **2005**, *109*, 6287-6293.

Hiyoshi, N.; Yogo, K.; Yashima, T. *Microporous Mesoporous Mater.* **2005**, *84*, 357-365.

Bacsik, Z.; Atluri, R.; Garcia-Bennett, A. E.; Hedin, N. *Langmuir* **2010**, *26*, 10013-10024.

Knöfel, C.; Martin, C.; Hornebecq, V.; Llewellyn, P. L. *J. Phys. Chem. C* **2009**, *113*, 21726-21734.

Tsuda, T.; Fujiwara, T.; Taketani, Y.; Saegusa, T. *Chem. Lett.* **1992**, 2161-2164.

Chang, A. C. C.; Chuang, S. S. C.; Gray, M.; Soong, Y. *Energy Fuels* **2003**, *17*, 468-473.

Khatri, R. A.; Chuang, S. S. C.; Soong, Y.; Gray, M. *Energy Fuels* **2006**, *20*, 1514-1520.

Khatri, R. A.; Chuang, S. S. C.; Soong, Y.; Gray, M. *Ind. Eng Chem. Res.* **2005**, *44*, 3702-3708.

Fisher II, J. C.; Tanthana, J.; Chuang, S. S. C. *Environ. Prog. Sustainable Energy* **2009**, *28*, 589-598.

Tanthana, J.; Chuang, S. S. C. *ChemSusChem* **2010**, *3*, 957-964.

Hao, S. Y.; Xiao, Q. A.; Yang, H.; Zhong, Y. J.; Pepe, F.; Zhu, W. D. *Microporous Mesoporous Mater.* **2010**, *132*, 552-558.

Leal, O.; Bolivar, C.; Ovalles, C.; Garcia, J. J.; Espidel, Y. *Inorg. Chim. Acta* **1995**, *240*, 183-189.

Huang, H. Y.; Yang, R. T.; Chinn, D.; Munson, C. L. *Ind. Eng. Chem. Res.* **2003**, *42*, 2427-2433.

Wang, X. X.; Schwartz, V.; Clark, J. C.; Ma, X. L.; Overbury, S. H.; Xu, X. C.; Song, C. S. *J. Phys. Chem. C* **2009**, *113*, 7260-7268.

Zheng, F.; Tran, D. N.; Busche, B. J.; Fryxell, G. E.; Addleman, R. S.; Zemanian, T. S.; Aardahl, C. L. *Ind. Eng. Chem. Res.* **2005**, *44*, 3099-3105.